

MultiTIME software (Phoenix Flow Systems).
31. Supported by grants from the USPHS. D.D. and K.L.H. contributed equally to this work. D.D. is supported by a fellowship from the Associazione Itali-

ana per la Ricerca sul Cancro (AIRC). S.A.M. is an American Cancer Society fellow. J.C.C. is an Ida and Cecil Green Professor of Cell Biology. We thank W. Jensen and C. Pleiman for helpful

advice and comments, and J. Franconi for secretarial assistance.

6 December 1994; accepted 15 February 1995

Activity-Dependent Action Potential Invasion and Calcium Influx into Hippocampal CA1 Dendrites

Nelson Spruston,* Yitzhak Schiller, Greg Stuart, Bert Sakmann

The temporal and spatial profile of activity-evoked changes in membrane potential and intracellular calcium concentration in the dendrites of hippocampal CA1 pyramidal neurons was examined with simultaneous somatic and dendritic patch-pipette recording and calcium imaging experiments. Action potentials are initiated close to the soma of these neurons and backpropagate into the dendrites in an activity-dependent manner; those occurring early in a train propagate actively, whereas those occurring later fail to actively invade the distal dendrites. Consistent with this finding, dendritic calcium transients evoked by single action potentials do not significantly attenuate with distance from the soma, whereas those evoked by trains attenuate substantially. Failure of action potential propagation into the distal dendrites often occurs at branch points. Consequently, neighboring regions of the dendritic tree can experience different voltage and calcium signals during repetitive action potential firing. The influence of backpropagating action potentials on synaptic integration and plasticity will therefore depend on both the extent of dendritic branching and the pattern of neuronal activity.

The prevailing view of how neurons function in the central nervous system is that synaptic potentials propagate passively to the soma, where they summate and, if the resulting depolarization is large enough, an action potential is initiated in the axon (1–5). In hippocampal CA1 pyramidal neurons, however, evidence exists both for somatic (3) and dendritic action potential initiation (6, 7). Once initiated, the extent to which action potentials depolarize the dendritic tree could influence neuronal function in a number of ways—for example, by summing with excitatory postsynaptic potentials (EPSPs) or by shunting the dendritic membrane. In CA1 pyramidal neurons, action potential-mediated depolarization can also result in the elevation of dendritic intracellular calcium concentration ($[Ca^{2+}]_i$) (8, 9), which is important for the induction of long-term changes in synaptic strength (10–12).

Simultaneous somatic and dendritic recordings (13) revealed that both the inflection point and the peak of action potentials evoked by threshold synaptic stimulation (Fig. 1A) or somatic or dendritic current pulses always occurred first at the soma (Fig. 1B). Similar results were observed for synaptically evoked action potentials recorded extracellularly in cell-attached patches (14). In a few cases, however, when synaptic stimulus intensities several times the

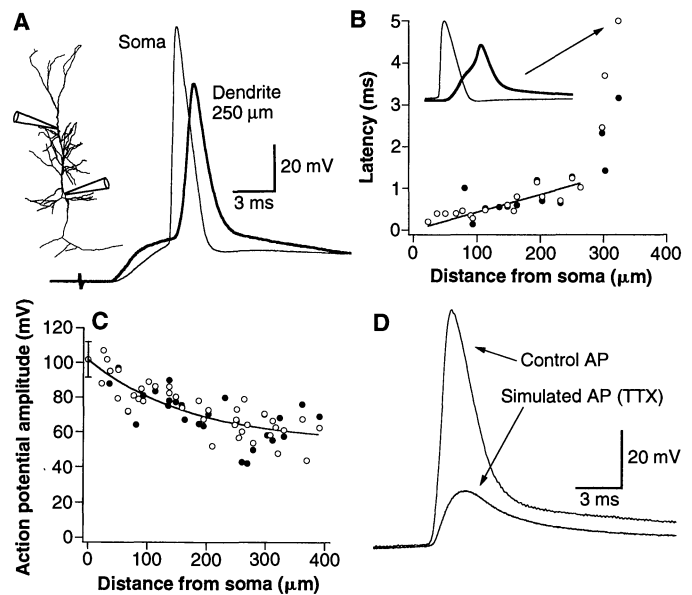
threshold value were used, the site of action potential initiation shifted into the proximal dendrites. Therefore the usual site of

tetrodotoxin (TTX)-sensitive action potential initiation in CA1 pyramidal neurons is near the soma (presumably in the axon) (3), but may shift into the proximal dendrites under some conditions (15). Such a shift may explain some previous reports of dendritic action potential initiation (6), but it is unclear whether such large, synchronous synaptic activation normally occurs in vivo.

The average conduction velocity of action potentials propagating from the soma back into the proximal 260 μm of the apical dendrites was 0.24 m/s (Fig. 1B). In the most distal simultaneous recordings (~300 μm from the soma), a longer latency was usually observed than would be expected from linear extrapolation of the closer points. This was due to a second inflection on the rising phase of the dendritic action potentials (Fig. 1B, inset). Action potentials in axons have a similar form when propagating close to threshold for failure of active propagation (16).

The amplitude of single action potentials measured with dendritic recordings at

Fig. 1. Action potentials are initiated near the soma and actively invade the dendrites of CA1 pyramidal neurons. **(A)** Action potentials recorded simultaneously from the soma (thinner line) and apical dendrite (thicker line) in response to synaptic stimulation. Note that the action potential occurs first in the somatic recording. The inset shows a camera lucida drawing of the neuron from which the recording was made at the locations indicated (lower pipette, soma). **(B)** Plot of the latency from the peak of the somatic action potential to the peak of the dendritic action potential as a function of distance of the recording site from the soma for all double recordings. Action potentials were evoked either by synaptic stimulation (filled circles) or current pulses (open circles). The straight line is a linear regression fit (forced to pass through the origin) to all points up to 264 μm from the soma, which indicates to a conduction velocity of 0.24 m/s. The inset (105 mV, 20 ms) shows the data for the indicated point. **(C)** Plot of spike amplitude (measured from the inflection point to the peak) as a function of distance of the recording site from the soma for action potentials evoked by either synaptic stimulation (filled circles) or dendritic current pulses (open circles). The somatic action potential amplitude is indicated by a single point (mean \pm SD, $n = 30$). The smooth line is an exponential fit to the data (somatic point weighted accordingly) with a distance constant of 170 μm . **(D)** Comparison of the amplitude of a simulated action potential (in the presence of 1 μM TTX) and a control action potential measured at the same dendritic location (210 μm). The simulated action potential was produced by using the action potential measured at the soma as a voltage-clamp command during somatic whole-cell voltage clamp (13).



Max-Planck-Institut für medizinische Forschung, Abteilung Zellphysiologie, Jahnstrasse 29, 69120 Heidelberg, Germany.

*To whom correspondence should be addressed.

distances of up to 390 μm from the soma decreased along the apical dendrite (Fig. 1C) (15). To investigate whether action potentials propagate actively into the dendrites, we compared the action potential in the dendrite to the dendritic voltage change observed when an action potential waveform was used as a somatic voltage-clamp command in the presence of 1 μM TTX (4). The amplitude of these passively propagating action potential waveforms was substantially less than that of control action

potentials at the same dendritic location (Fig. 1D) ($n = 4$), demonstrating that the backpropagation of action potentials into the dendritic tree of CA1 pyramidal neurons is actively supported by dendritic voltage-gated Na^+ channels (9, 17, 18).

CA1 pyramidal neurons can fire bursts of action potentials in vivo (19), and high-frequency activation of these neurons can induce changes in synaptic strength (10, 11). We therefore investigated the propagation of action potentials into the den-

drites during trains of action potentials. Somatic and dendritic recordings showed that dendritic action potential amplitude decreased during a train, whereas somatic action potentials did not attenuate significantly (Fig. 2, A and B) ($n = 25$; 12 double recordings and 13 single-site dendritic recordings). Similar results were observed in cell-attached patches (Fig. 2C) ($n = 4$) (14). The ratio of the last to the first action potential amplitude in a 1-s train of 10 to 20 action potentials decreased significantly with distance from the soma (Fig. 3A). At the most distal dendritic recording sites ($>300 \mu\text{m}$), action potential amplitude often decreased abruptly after the first few action potentials in a train (20) (Figs. 2 and 3, B to D), indicating that the first few action potentials propagate actively throughout the entire dendritic tree, but induce a change such that later action potentials in the train fail to efficiently propagate into the distal dendrites.

Subthreshold depolarizations did not result in attenuation of a test action potential occurring 200 ms after the 1-s-long depolarization (Fig. 3B, right trace). Suprathreshold depolarization, however, resulted in attenuation of action potential amplitude during the train, with the test action potential remaining small for a longer time when more action potentials were evoked (Fig. 3B, compare left and middle traces). These results indicate that the amount of depolarization determines the extent and duration of activity-dependent action potential propagation. In proximal dendritic recordings, the time course of recovery of action potential amplitude after a 1-s train of action potentials was usually gradual, requiring a few seconds for complete recovery. In distal dendritic recordings ($>300 \mu\text{m}$), however, recovery occurred in two phases: An initial, sudden increase in amplitude within 500 ms after the train, followed by a second, slower phase, usually requiring a few seconds to reach control amplitude (Fig. 3C) ($n = 5$). The recovery of action potential amplitude could be accelerated by hyperpolarization at the end of the train (Fig. 3D). The time and voltage dependence of the induction and recovery of activity-dependent action potential attenuation suggests that activation or inactivation of voltage-gated channels in the dendrites underlies this process.

The abrupt decrease in action potential amplitude during a train of action potentials recorded in the distal dendrites and the corresponding abrupt increase during the recovery of action potential amplitude suggest that a transition occurs between active and passive propagation of action potentials into the distal dendrites. Furthermore, branch points are a known point of weakness for active propagation of action poten-

Fig. 2. Action potential invasion of CA1 pyramidal neuron dendrites is activity-dependent. **(A)** Trains of action potentials evoked by somatic current injection in simultaneous somatic and dendritic recordings from the two neurons shown at the locations indicated by the arrows. Action potentials were evoked by 200 pA (left cell) or 70 pA (right cell) current injection through the somatic pipette. The train of somatic action potentials in the left cell was similar to that shown for the right cell (little attenuation during the train). **(B)** Action potentials evoked in the soma (lower trace) and dendrite (upper trace) by synaptic stimulation (16 Hz, 1 s) in the same cell shown at the right in (A). **(C)** Currents measured in two dendritic cell-attached patches during suprathreshold synaptic stimulation (16 Hz, 1 s) (top and middle traces). The intracellular membrane potential from the same dendrite as the middle trace is shown in the lower trace (separate recordings from the same location, with similar synaptic stimulation). The stimulus artefacts in (B) and (C) are truncated.

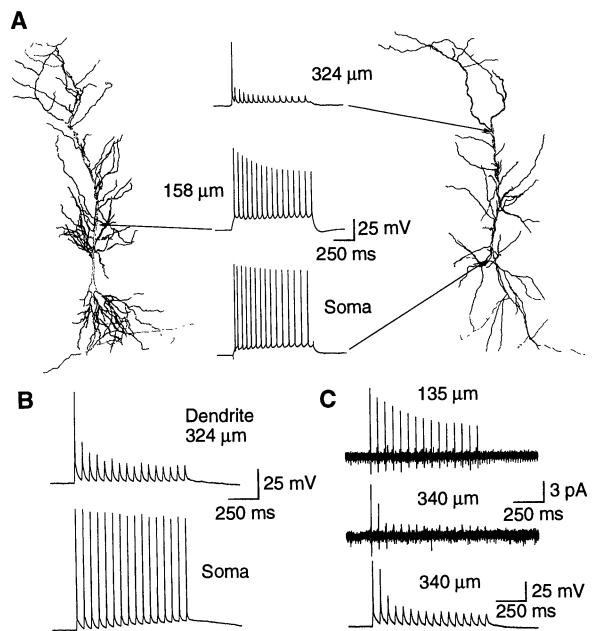
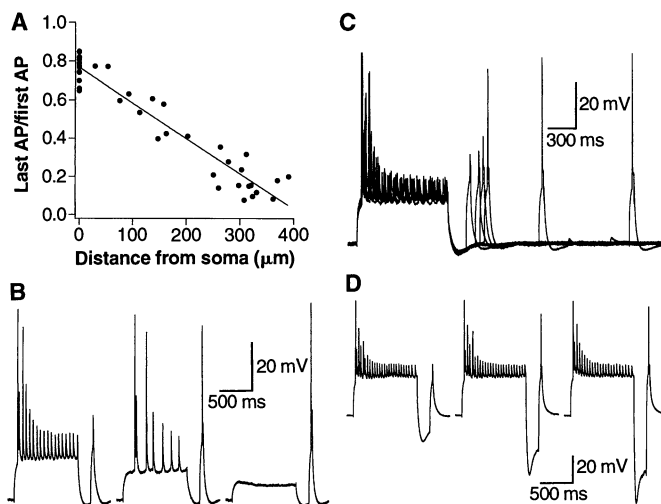


Fig. 3. Properties of activity-dependent action potential attenuation in CA1 pyramidal neuron dendrites. **(A)** Plot of the ratio of the action potential amplitude of the last to the first action potential in a train (10 to 20 action potentials during a 1-s current pulse) as a function of distance of the recording site from the soma. **(B)** Attenuation of a test action potential depends on the amount of prior depolarization. Conditioning current injections were 120, 70, and 50 pA (left to right), for 1 s. Test action potentials were evoked by a 130 pA, 50 ms current pulse. **(C)** Recovery of action potential amplitude after a train of action potentials. Conditioning current injections were 130 pA, 1 s. Test action potentials were evoked by 200 pA, 50 ms current pulses at different times after the conditioning pulse. **(D)** Recovery of action potential amplitude is accelerated by hyperpolarization. Trains of action potentials were evoked by current pulses of 200 pA, 1 s. Hyperpolarizing current pulses were -100 , -300 , and -500 pA (left to right), for 200 ms. Test action potentials were evoked by 200 pA, 50 ms current pulses. Data in (B) through (D) are all from the same dendritic recording, 317 μm from the soma.



tials in axons (21). We therefore investigated the possibility that failure of active action potential backpropagation occurs at dendritic branch points. As the entire dendritic tree of CA1 pyramidal neurons contains voltage-activated Ca^{2+} channels (9), Ca^{2+} imaging experiments (22) were used to examine the relative effectiveness of invasion of single and trains of action potentials at dendritic branch points (Fig. 4). We observed examples where the $[\text{Ca}^{2+}]_i$ transient evoked by a train of action potentials was substantially reduced at a branch point, whereas that evoked by a single action potential was comparatively unaltered (Fig. 4B). This result, observed in 64% of all neurons mapped (23), suggests that the failure of active propagation of action potentials into the dendritic tree during a train of action potentials can occur at branch points. Furthermore, in the example shown in Fig. 4B, the $[\text{Ca}^{2+}]_i$ signal evoked by a train of action potentials differed significantly between the two branches ($n = 3$) (23).

The activity-dependent attenuation of action potential amplitude in the dendrites of hippocampal CA1 pyramidal neurons appears to arise as a consequence of three factors. First, the efficiency of active action potential backpropagation is low enough that the amplitude of a single action potential decreases slightly as it propagates into the dendrites. Second, the development of a time- and voltage-dependent process during a train of action potentials appears to reduce this efficiency further. Third, the safety factor for backpropagation of action potentials is low at dendritic branch points. We suggest that a gradual reduction in the capacity for active action potential invasion of the dendrites occurs during a train of action potentials and that this process can ultimately lead to failure of active propagation at branch points. Processes that could contribute to this failure include inactivation of dendritic voltage-gated Na^+ or Ca^{2+} channels or shunting of the dendritic membrane by voltage- or Ca^{2+} -activated K^+ or Cl^- channels (24).

A consequence of the activity-dependent reduction of action potential backpropagation is that the spatial profile of $[\text{Ca}^{2+}]_i$ signals in the dendrites evoked by single and trains of action potentials is likely to differ. We therefore examined changes in $[\text{Ca}^{2+}]_i$ evoked by single and trains of action potentials at multiple sites within the dendritic tree of CA1 pyramidal neurons. Although the $[\text{Ca}^{2+}]_i$ transient evoked by single action potentials was not significantly different along the entire apical dendritic tree (Fig. 5, A and B) (25), on average the $[\text{Ca}^{2+}]_i$ transient evoked by a train of action potentials decreased substantially with distance from the soma (Fig. 5, A and C). A decrease of the $[\text{Ca}^{2+}]_i$ transient

evoked by a train of action potentials with distance from the soma has also been observed by Jaffe *et al.* (9). The improved spatial resolution in our experiments revealed that this reduction was spatially heterogeneous, with a large variability in the amplitude of $[\text{Ca}^{2+}]_i$ transients evoked by trains of action potentials in different dendritic sites (Fig. 5, A and C). In the example in Fig. 5A, a small reduction in the peak $[\text{Ca}^{2+}]_i$ transient evoked by a train of action potentials is seen at the first major branch

point, followed by a marked reduction in a more distal branch point. Consequently, a train of action potentials results in $[\text{Ca}^{2+}]_i$ signals that differ substantially in two adjacent dendritic branches, even at similar distances from the soma (compare the left and right top traces in Fig. 5A). The dendritic profile of $[\text{Ca}^{2+}]_i$ transients evoked by single and trains of action potentials is consistent with the picture of activity-dependent invasion of action potentials into CA1 dendrites that emerges from the

Fig. 4. Calcium imaging reveals failure of activity-dependent backpropagating action potentials at a dendritic branch point in a CA1 pyramidal neuron. **(A)** Dendritic $[\text{Ca}^{2+}]_i$ (upper traces) and somatic membrane potential (lower traces) recorded during a single action potential (black line, smaller peak) and a train of action potentials (gray line, larger peak, 16 Hz, 500 ms). $[\text{Ca}^{2+}]_i$ transients were recorded from a dendritic region of interest marked by the lower arrow in **(B)**. **(B)** Image of the neuron (under resting conditions) shows a branch point located 180 μm from the soma. $[\text{Ca}^{2+}]_i$ transients evoked by single (black lines, smaller peaks) and trains (gray lines, larger peaks) of action potentials (16 Hz, 500 ms) were measured from regions of interest indicated by the white arrows. The ratio of the peak calcium transients evoked by a train and single action potentials (CT16/CT1) was not significantly different between the two regions of interest measured proximal to the bifurcation (CT16/CT1 = 4.1 and 4.3) and only slightly reduced in the region of interest measured in the right branch (CT16/CT1 = 3.4). In contrast, a marked reduction was observed in the left branch (CT16/CT1 = 1.1).

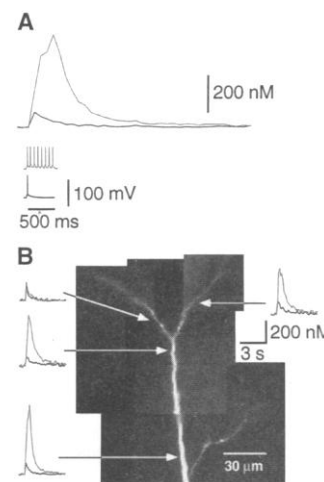
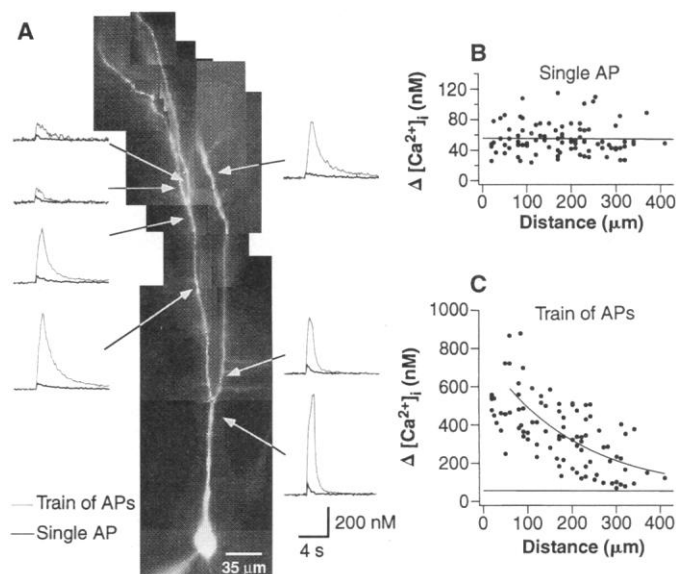


Fig. 5. Activity-dependent heterogeneity of dendritic $[\text{Ca}^{2+}]_i$ transients in CA1 pyramidal neurons. **(A)** Image of the neuron (under resting conditions) with $[\text{Ca}^{2+}]_i$ transients evoked by single (black lines, smaller peaks) and trains (gray lines, larger peaks) of action potentials (16 Hz, 1 s) recorded from regions of interest indicated by the white arrows. Whereas $[\text{Ca}^{2+}]_i$ transients evoked by a single action potential were similar at all locations, those evoked by a train of action potentials showed significant spatial differences within the dendritic tree. Note the large reduction in the amplitude of the $[\text{Ca}^{2+}]_i$ transients evoked by trains of action potentials just distal to the second major branch point (left), compared to the other distal region of interest located at a similar distance from the soma (right). **(B)** $\Delta[\text{Ca}^{2+}]_i$ (peak minus baseline) evoked by single action potentials plotted as a function of distance from the soma. The values were obtained from 20 neurons, and the points were fit with a linear function (slope of $-0.003 \text{ nM}/\mu\text{m}$). **(C)** $\Delta[\text{Ca}^{2+}]_i$ evoked by trains of action potentials (16 Hz, 1 s) plotted as a function of distance from the soma. Note the large variability in the values measured at similar distances from the soma, presumably reflecting large variation in the propagation efficiency of a train of action potentials into different dendritic branches. The smooth line is an exponential fit to the data with a distance constant of 200 μm . Only the points starting from the maximum $\Delta[\text{Ca}^{2+}]_i$ values (50 μm from the soma, as determined by binning the data) are fit. The linear fit obtained for the single action potential amplitudes (B) is plotted for comparison.



voltage recordings described above. Furthermore, the spatial heterogeneity in the $[Ca^{2+}]_i$ transients evoked by trains of action potentials suggests that different dendritic branches experience different voltage changes during repetitive action potential firing.

Backpropagation of somatic action potentials into the dendritic tree, which also occurs in neocortical pyramidal neurons (4), may convey the activity level of the neuron to dendritic synapses. One candidate for the effector of such a signal could be Ca^{2+} influx into the dendrites, occurring through either voltage-gated Ca^{2+} channels (8, 9, 26) or *N*-methyl-D-aspartate (NMDA) receptor channels at activated synapses (27). Here we demonstrate that in contrast to previous reports (9, 18), single action potentials can invade the distal dendrites of CA1 neurons and result in a substantial elevation of $[Ca^{2+}]_i$. This finding suggests that active backpropagation of action potentials is supported by voltage-gated Na^+ channels distributed over the entire apical dendrite, consistent with recent cell-attached patch-clamp recordings from the dendrites of CA1 neurons (28). We also demonstrate, however, that activation of distal dendritic Ca^{2+} channels during trains of action potentials is limited by an activity-dependent process (9) that can ultimately result in failure of action potential backpropagation at dendritic branch points.

Such propagation failures may confer the dendritic tree with computational properties, by allowing branch points to act as "gates" that control the number of action potentials propagating actively into individual dendritic branches. Such gates need not act symmetrically (Fig. 4B) and might be under dynamic control by synaptic or neuromodulatory inputs. For example, synaptic inhibition could increase the effectiveness of backpropagation at specific branch points, in a similar way to that observed after membrane hyperpolarization (Fig. 3D).

These findings have implications for synaptic integration and plasticity, as synapses located at different distances from the soma and on different branches at the same distance will experience very different voltage and Ca^{2+} signals during repetitive action potential firing. If backpropagating action potentials are involved in the induction of some forms of synaptic plasticity, such as potentiation produced by depolarization alone (12) or pairing of pre- and postsynaptic activity (10), synapses on different dendritic branches would be differentially susceptible to such potentiation. On the other hand, activity-dependent failure of action potential backpropagation may facilitate the synapse specificity of long-term potentiation

by limiting the extent of generalized increases in dendritic $[Ca^{2+}]_i$ during high-frequency synaptic activation (29).

REFERENCES AND NOTES

1. J. C. Eccles, *The Physiology of Synapses* (Springer-Verlag, Berlin, 1964).
2. J. G. R. Jefferys, *J. Physiol. (London)* **289**, 375 (1979).
3. T. L. Richardson, R. W. Turner, J. J. Miller, *J. Neurophysiol.* **58**, 981 (1987).
4. G. J. Stuart and B. Sakmann, *Nature* **367**, 69 (1994).
5. G. J. Stuart and M. Häusser, *Neuron* **13**, 703 (1994).
6. Y. Fujita and H. Sakata, *J. Neurophysiol.* **25**, 209 (1962); P. Andersen, *Acta Physiol. Scand.* **48**, 178 (1960); P. Andersen, B. Holmqvist, P. E. Voorhoeve, *ibid.* **66**, 461 (1966); P. Andersen and T. Lomo, *Exp. Brain Res.* **2**, 247 (1966); O. Herreras, *J. Neurophysiol.* **64**, 1429 (1990).
7. B. G. Cragg and L. H. Hamlyn, *J. Physiol.* **129**, 608 (1955); W. A. Spencer and E. R. Kandel, *J. Neurophysiol.* **24**, 272 (1961); R. K. S. Wong, D. A. Prince, A. I. Basbaum, *Proc. Natl. Acad. Sci. U.S.A.* **76**, 986 (1979); N. P. Poolos and J. D. Kocsis, *Brain Res.* **524**, 342 (1990); S. B. Colling and H. V. Wheal, *Neurosci. Lett.* **172**, 73 (1994).
8. W. G. Regehr, J. A. Connor, D. W. Tank, *Nature* **341**, 533 (1989).
9. D. B. Jaffe *et al.*, *ibid.* **357**, 244 (1992).
10. B. Gustafsson, H. Wigström, W. C. Abraham, Y.-Y. Huang, *J. Neurosci.* **7**, 774 (1987).
11. T. V. P. Bliss and G. L. Collingridge, *Nature* **361**, 31 (1993); L. M. Grover and T. J. Teyler, *ibid.* **347**, 447 (1990); D. Johnston, S. Williams, D. Jaffe, R. Gray, *Annu. Rev. Physiol.* **54**, 489 (1992).
12. D. M. Kullmann *et al.*, *Neuron* **9**, 1175 (1992).
13. Patch-pipette recordings were obtained from the soma and dendrites of CA1 pyramidal neurons in transverse hippocampal slices (300 μ m thick) from 13- to 32-day-old Wistar rats (mostly 28 days) as described [G. J. Stuart, H.-U. Dodt, B. Sakmann, *Pflügers Arch.* **423**, 511 (1993)]. The extracellular solution consisted of 125 mM NaCl, 25 mM glucose, 2.5 mM KCl, 1.25 mM NaH_2PO_4 , 2 mM $CaCl_2$, and 1 mM $MgCl_2$ (pH 7.4, bubbled with 95% O_2 , 5% CO_2). Patch-pipettes were filled with 115 mM potassium gluconate, 20 mM KCl, 10 mM EGTA, 10 mM sodium phosphocreatine, 10 mM Hepes, 4 mM magnesium adenosine triphosphate (MgATP), 0.3 mM guanosine triphosphate (GTP), creatine phosphokinase (50 U/ml), and in most cases biocytin (5 mg/ml), and had open-tip resistances of 5 to 10 megohms. Whole-cell patch-pipette recordings were made with Axoclamp 2B amplifiers (Axon Instruments) with appropriate bridge and capacitance compensation. Series resistance was 10 to 100 megohms. Recordings were terminated if series resistance exceeded 100 megohms. Most recordings were made at room temperature (22° to 24°C), but all findings were confirmed at 35° to 37°C ($n = 6$). Similar results were also obtained with 0.5 mM EGTA in the pipette solution. On average, resting potentials did not differ in somatic and dendritic recordings [-62 ± 1 mV (mean \pm SEM), $n = 25$ somatic recordings; -62 ± 1 mV, $n = 41$ dendritic recordings]. Synaptic stimulation was performed by placing a stimulating electrode (monopolar carbon fiber or bipolar tungsten wire) in the stratum radiatum (biphasic pulses, 5 to 50 V, 100 to 1000 μ s). In simulated action potential experiments (Fig. 1D), an EPC-7 patch-clamp amplifier (List Electronics) was used for the somatic recording in both current- and voltage-clamp modes. Series resistance during somatic whole-cell voltage clamp was 5 to 8 megohms (compensated by more than 70%). Cell-attached patch recordings were performed in continuous voltage clamp with either Axoclamp 2B or EPC-7 amplifiers.
14. The use of cell-attached patch recordings rules out the possibility that the findings are caused by wash-out of cytoplasmic constituents or capacitance loads imposed on the cell by the patch pipettes.
15. R. W. Turner, D. E. R. Meyers, T. L. Richardson, J. L. Barker, *J. Neurosci.* **11**, 2270 (1991).
16. C. Lüscher, J. Streit, R. Quadroni, H.-R. Lüscher, *J. Neurophysiol.* **72**, 622 (1994).
17. H. Miyakawa and H. Kato, *Brain Res.* **399**, 303 (1986).
18. R. W. Turner, D. E. R. Meyers, J. L. Barker, *J. Neurophysiol.* **62**, 1375 (1989).
19. B. H. Bland and L. V. Colom, *Prog. Neurobiol.* **41**, 157 (1993).
20. In 9 of 11 recordings at distances greater than 300 μ m an abrupt decrease in action potential amplitude was observed (greater than 50% of the total decrease occurred between two successive action potentials), whereas the other two recordings more distal than 300 μ m and 14 recordings between 30 and 280 μ m showed a more gradual decrease in action potential amplitude during the train.
21. S. S. Goldstein and W. Rall, *Biophys. J.* **14**, 731 (1974).
22. CA1 pyramidal neurons were loaded by means of a somatic patch pipette containing 115 mM potassium gluconate, 20 mM KCl, 10 mM sodium phosphocreatine, 10 mM Hepes, 2 mM MgATP, 2 mM sodium ATP, 0.3 mM GTP, and 150 μ M fura-2 (Molecular Probes). Action potentials were elicited by single or trains of 25-ms current injections and the resulting fluorescence was collected at 10 Hz from well-focused regions of interest (10 to 25 μ m long, 5 to 12 μ m wide) with a cooled slow-scan charge-coupled device camera (CH250A, Photometrics) mounted on an upright epifluorescence microscope (Axioscop FS, Zeiss), equipped with a 63 \times water-immersion objective (Achromplan, Zeiss). Background fluorescence was subtracted, bleach correction performed, and fluorescent values (averages of four to five responses) converted to $[Ca^{2+}]_i$ with the isosbestic ratio method as described (26).
23. $[Ca^{2+}]_i$ transients evoked by single and trains of action potentials were examined in a total of 20 cells, but imaging of the distal dendrites (beyond 200 μ m from the soma) was possible in only 17 cells. Failure of action potentials to propagate into apical dendrites during a train was inferred to have occurred (14 out of 17 neurons) if the ratio of the peak of the $[Ca^{2+}]_i$ transient produced by a train of 16 action potentials to the peak of the $[Ca^{2+}]_i$ transient produced by a single action potential (CT16/CT1) was reduced in the distal dendrites to less than one-third of its value in the proximal dendrites (50 to 100 μ m from the soma). In 11 of these 14 neurons, an attempt was made to determine whether the failure was localized (classified as a twofold reduction in CT16/CT1 over a distance of 60 μ m or less between the center of two adjacent regions of interest). Localized failures that correlated with a major branch point were observed in 7 of these 11 cases (64%); in the other 4 neurons the reduction was more gradual, but localized reductions may have occurred at sites that were not imaged. In 5 of these 7 neurons, both dendrites arising from the branch point were imaged and differential invasion of the two branches was observed in three cases. By "major" branch points, we mean clear bifurcations of the main apical dendrite, as opposed to points where oblique branches arise from the main apical dendrite.
24. C. Lüscher, J. Streit, P. Lipp, H.-R. Lüscher, *J. Neurophysiol.* **72**, 634 (1994).
25. Because of the larger surface to volume ratio of distal dendrites, this finding implies that single action potentials evoke less Ca^{2+} influx distally, consistent with the attenuation of action potential amplitude along the apical dendrite.
26. J. Schiller, F. Helmchen, B. Sakmann, *J. Physiol. (London)*, in press.
27. N. Spruston, P. Jonas, B. Sakmann, *ibid.* **482**, 325 (1995).
28. J. C. Magee and D. Johnston, *ibid.*, in press.
29. W. G. Regehr and D. W. Tank, *J. Neurosci.* **12**, 4202 (1992); D. J. Perkel, J. J. Petrozzino, R. A. Nicoll, J. A. Connor, *Neuron* **11**, 817 (1993); R. Malinow, N. Otmakhov, K. I. Blum, J. Lisman, *Proc. Natl. Acad. Sci. U.S.A.* **91**, 8170 (1994).
30. We thank C. Racca for doing the camera lucida drawings and J. C. Magee for comments on the manuscript. Supported by the Max-Planck-Gesellschaft, the Alexander von Humboldt Foundation (N.S. and G.S.), and the Minerva Foundation (Y.S.).

16 December 1994; accepted 22 February 1995